

Investigation of Cu²⁺ Hydration and the Jahn–Teller Effect in Solution by QM/MM Monte Carlo Simulations

Gerhard W. Marini, Klaus R. Liedl, and Bernd M. Rode*

Department of Theoretical Chemistry, Institute for General, Inorganic and Theoretical Chemistry, University of Innsbruck, A-6020 Innsbruck, Austria

Received: June 17, 1999; In Final Form: October 18, 1999

The Cu²⁺ hydration shell structure has been studied by a combined ab initio quantum mechanical/molecular mechanical (QM/MM) Monte Carlo simulation, in which the ion and its first hydration sphere are treated at the Born–Oppenheimer ab initio quantum mechanical level, while classical pair and three-body potentials are employed for the remaining system. Whereas traditional simulations based on MM potentials are not able to predict higher-body effects such as the Jahn–Teller (JT) distorted octahedral structure of the first hydration shell of Cu²⁺, the combined QM/MM approach reproduces correctly this experimentally confirmed property and delivers more accurate hydration energy values as well.

1. Introduction

Because of its widespread and important role in condensed phase chemistry and biochemistry^{1–4} numerous experimental and theoretical^{5–14} investigations have focused on the structural properties of hydrated cupric ion, Cu²⁺. The most powerful experimental methods for structural elucidation are X-ray¹⁵ and neutron diffraction, together with NMR and quasielastic neutron scattering.^{16–18} Such studies on various copper(II) salts have provided considerable insight into the surroundings of Cu²⁺ in water.^{19–21} There is strong experimental evidence for a JT distortion of the hexaquo complex which is best represented by a model where two bonds are elongated, leading to a tetragonal bipyramidal structure with four closer equatorial and two more distant axial ligands.

The experimental methods, however, quickly reach their limits. Sophisticated modeling techniques and structural assumptions required to interpret experimental data often lead to contradictory results for ionic complex structures, particularly ions such as Cu²⁺,²¹ display a more “labile” character of the water ligands, which is attributed to the dynamics of the JT effect as the “short” and “long” bonds in the [Cu(H₂O)₆]²⁺ complex are changing in favor of water exchange at the more distant axial sites. Hence, in aqueous solution the solvent–ligand exchange rate is much faster for Cu²⁺ than for most other ions of similar size and charge and has not yet been determined unambiguously.^{10,22,23} Water exchange rates not accessible to experimental observation imply that only mean values of the composition of the metal ion’s coordination shell can be derived. However, the exact composition and distribution of all microspecies could eventually be elucidated by means of computer simulations allowing identification of all distinct microspecies present.

The importance of considering the hydrogen bond network in water beyond the highly oriented primary and the less ordered second solvation shell is supported by a recent study²⁴ using electrospray to generate gas-phase [Cu(H₂O)_n]²⁺ clusters which implies that at $n = 8$ the most stable complex is formed, in contrast to the well-established view of a JT distorted hexaquo copper species in solution.

To describe an n -body system exactly, the intermolecular interactions have to be written as a sum of 2, 3, ..., up to n -body terms. Using the rather rough assumption of pairwise additive intermolecular potentials and thus neglecting many-body interactions, Monte Carlo simulations for some mono- and divalent metal ions have led to structural results in agreement with those achieved experimentally.^{25–27} In most cases concerning small monovalent, divalent, and trivalent ions, however, this simplification results in wrong structural properties of the solvate and errors in energies of 10–15%. Consequently, even rough data as first-shell coordination numbers are predicted much higher than found by experiment, as for example in the case of Li⁺,²⁸ Na⁺,²⁹ or K⁺,²⁹ Be²⁺,^{30,31} Fe²⁺,³² Fe³⁺,³³ Ni²⁺,^{34,35} and Cu²⁺.^{36–38} In the latter case, ab initio studies of successive hydration have indicated that three-body and even higher terms should be of major importance to correctly characterize this ion in aqueous solution.^{33,39}

The problem of the failure of pairwise additivity for cation–water potentials, especially for doubly and triply charged cations, can be dealt with in several ways. To limit the computational effort one approach is to define effective pair potentials³⁸ which consider mean many-body effects to a certain extent in an empirical way. For example, simulations performed with the so-called “nearest neighbor ligand correction” (NNLC) algorithm for aqueous solutions of CuCl₂,^{36,40,41} Zn²⁺,⁴² and ZnCl₂⁴³ include, in addition to pair potential terms, a three-body correction term based on ab initio calculations. SCF-MO computations at the Hartree–Fock level using ECP-DZP basis sets were performed to describe the molecular energy surface of the metal ion monohydrate interacting with another water molecule or the anion.

A more rigorous and exact approach is to supplement the potential energy function to be employed in simulations with higher-body terms. In several cases, three-body potentials, obtained from ab initio methods at the level specified above, have been found adequate to reproduce properly hydration numbers.^{29–33,35–38,44–46} The cost and complexity of the calculations and fitting procedures increase with the order of the n -body terms to be determined⁴⁷ by ab initio methods and they are, therefore, hardly feasible for larger systems and n larger than 3.

This dilemma has motivated the development of hybrid models for combined QM/MM approaches^{48–51} in which a subsystem of particular interest, e.g. the solvation shell around a solute molecule is treated quantum mechanically, while the environment consisting of solvent molecules is approximated by molecular mechanics potentials. These models are guided by the general idea that the chemical system may be partitioned into a strongly interacting region which requires quantum mechanical treatment and a remainder where the weaker interactions allow a classical MM description.

This approach has already been successfully employed within the molecular dynamics and Monte Carlo scheme,⁵² with the quantum subsystem described at the Hartree–Fock⁵³ or density functional level of theory.^{54,55} Aqueous solutions of organic molecules,^{56,57} as well as ionic hydration,^{53,58–62} have been treated by a combined QM/MM approach.

In the present work, a combined quantum mechanical and molecular mechanics formalism has been developed and implemented in a Monte Carlo simulation program⁶³ in order to investigate the importance of nonadditive terms for the hydration of Cu²⁺. Within this approach an area of particular chemical interest in the elementary box is defined as the QM area and treated by ab initio calculations whenever a particle within its boundary is moved. The remaining system contributes classically by means of pair and three-body potentials to the overall system energy. Especially designed to provide a quantitative prediction of solvation phenomena, the QM area comprises the ion itself and all ligands bound within the first coordination sphere. Particular attention has to be paid to particles migrating across the boundary between the QM and MM area. To achieve a steady transition from quantum chemical to classical energy contributions, the relevant interactions have to be gradually changed by a smoothing function. Since the force calculations required for molecular dynamics simulations consume roughly 3 times more CPU time than comparable energy calculations, hybrid Monte Carlo approaches should be especially useful for extracting structural and thermodynamical data at lower computational cost.

2. Methodology

According to Warshel et al.⁴⁸ and in the formulation of Field et al.⁵⁰ the combined QM/MM treatment involves a partitioning of effective Hamiltonian of the system into three terms:

$$\hat{H}_{\text{eff}} = \hat{H}_{\text{QM}}^0 + \hat{H}_{\text{QM/MM}} + \hat{H}_{\text{MM}}$$

where \hat{H}_{QM}^0 is the Hamiltonian of the QM region, \hat{H}_{MM} represents the interaction energy between solvent molecules in the MM area and $\hat{H}_{\text{QM/MM}}$ the QM/MM interaction Hamiltonian which couples the solvent effects with QM calculations and ensures a smooth transition between QM and MM regions. Having defined the effective Hamiltonian, the total energy at an instantaneous configuration sampled during a MC simulation is determined by the expectation value of the wave function Φ ,

$$E_{\text{tot}} = \langle \Phi | \hat{H}_{\text{eff}} | \Phi \rangle = E_{\text{QM}}^0 + E_{\text{QM/MM}} + E_{\text{MM}}$$

whereby E_{QM}^0 refers to the energy of the particles in the QM sphere defined by the radius R_{on} and E_{MM} is the MM force field for interactions among the solvent molecules with larger distances than R_{off} defined by the limit of the transition region. $E_{\text{QM/MM}}$ contains distance-dependent parts of the QM ($E_{\text{QM}}^{\text{TR}}$) as well as the MM ($E_{\text{MM}}^{\text{TR}}$) energies assigned to the particles within the transition region:

$$E_{\text{QM/MM}} = f_{\text{SW}}(r_i)E_{\text{QM}}^{\text{TR}} + (1 - f_{\text{SW}}(r_i))E_{\text{MM}}^{\text{TR}}$$

$$r_i < R_{\text{on}} \Rightarrow f_{\text{SW}}(r_i) = 1$$

$$R_{\text{on}} \leq r_i \leq R_{\text{off}} \Rightarrow f_{\text{SW}}(r_i) = \frac{(R_{\text{off}} - r_i)^2(R_{\text{off}} + 2r_i - 3R_{\text{on}})}{(R_{\text{off}} - R_{\text{on}})^3}$$

$$r_i > R_{\text{off}} \Rightarrow f_{\text{SW}}(r_i) = 0$$

where r_i denotes the distance of mass of ligand i from the solute molecule in the center of the spherical region treated by QM methods, and $f_{\text{SW}}(r_i)$ is a smoothing function⁶⁴ that ensures that the energies change continuously at the boundaries of the regions, thus being essential for proper energy conservation.

The full ab initio computation of the first shell particles at HF level of accuracy leads to a substantial improvement compared to the description by classical potentials only which have been derived from ab initio calculations of comparable quality. The quantum chemical treatment of the hydrated metal ion does not only include all many-body effects within this region but additionally avoids the errors inherent to the fitting process of the analytical potential functions. For the study presented here, the code of our Monte Carlo program⁶³ has been combined with an interface to the energy calculation routines of the GAUSSIAN94⁶⁵ and GAUSSIAN98⁶⁶ programs, respectively.

3. Details of Calculation

All Monte Carlo simulations were carried out for the NVT ensemble, consisting of one Cu²⁺ ion and 399 water molecules in the periodic cube at a temperature of 298.16 K. A spherical cutoff of half of the box length was applied. Although the density was assumed to be the same as in pure water (0.997 g/cm³), the conditions of the system do not refer exactly to an infinitely dilute solution due to the applied periodic boundary condition. The edge length of the box was 22.94 Å. First, a classical simulation was performed using the following analytical potentials: for water–water interactions the CF2 potential⁶⁷ was used as this water model appeared more appropriate than the MCY⁶⁸ model for ion–water interactions;⁶⁹ a pair plus three-body potential³⁷ has been employed to account for the copper(II)–water. The starting configuration was obtained by random generation, and 3 million configurations were needed until the system reached equilibrium. The sampling of another 3 million configurations provided the reference data for the succeeding computations.

The QM/MM Monte Carlo simulation was started from the resulting equilibrium configuration. The quantum chemical calculations were carried out at the restricted open-shell Hartree–Fock level, while the remaining system was treated by the previously employed pair and three-body potentials. For Cu²⁺, basis set derived from Ahlrichs' DZV basis set⁷⁰ has been used, modified in a TZ type fashion according to the authors' recommendation to give a more balanced description of the ion's valence shells. The ECP-DZP basis set of Dunning and Huzinaga⁷¹ was employed for water whose geometry was kept rigid with an O–H distance of 0.9601 Å and an H–O–H angle of 104.47°. ⁷² Since the quantum mechanical energy calculations are very demanding, the size of the corresponding sphere must not be too large, but certainly had to include the first hydration shell. On the basis of previous classical Monte Carlo simulations^{37,73} and our reference simulation, the radius R_{on} was chosen to be 3.0 Å, smoothing was applied within an interval of 0.2 Å up to the outer boundary radius R_{off} of 3.2 Å. Ab initio energy

calculations were only performed when particles within the boundaries of the quantum mechanically treated sphere changed their position, thus reducing the computational effort drastically. After generating 0.5 million configurations the system had reached energetic equilibrium. For the evaluation of structural data, 3 million more configurations were generated and sampled every 800th step. The quantum mechanical calculations and the simulations were performed on a SGI Power Challenge workstation of the computer center of the University of Innsbruck. Overall, 49,960 ab initio calculations had to be performed within the framework of these simulations, requiring 256.6 days of CPU time.

4. Results and Discussion

4.1. Many-Body Interactions. The necessity of taking into account three-body effects for Cu²⁺–water interactions for potentials has been pointed out in previous studies.³⁷ Although the main contributions of these three-body effects are generated within the first hydration shell, nonadditivity still plays a significant role at farther distances than the R_{off} value considered here and is thus not negligible for an accurate description of more subtle solvation effects. Between 85.0% and 95.4% (average $91.7 \pm 1.3\%$) of the three-body energies are covered by the quantum mechanical treatment of the first hydration shell of the Cu²⁺ ion. Accordingly, the potentials used for the remaining system had to contain explicit three-body terms for copper–water interactions up to distances of 6 Å. Accordingly, higher-body effects stabilize the [Cu(H₂O)₆]²⁺ species by an average energy contribution of 22.2 kcal/mol, clearly revealing the presence of many-body effects beyond three-body interactions.

4.2. Structural and Thermodynamic Data. The structural data of the hydrated copper ion will be discussed in terms of radial density functions (RDFs) and coordination number, energy, and angular distributions.

The RDFs for copper–oxygen and copper–hydrogen, obtained from the combined QM/MM and the corresponding MM simulation, are shown in Figure 1 together with their running integration numbers. In the QM/MM simulation, the first peak of the Cu²⁺–O RDF is centered at 2.08 Å. The second peak of this function related to the second hydration shell appears between 3.3 and 4.9 Å with a maximum value at 4.2 Å, clearly separated from the first coordination sphere. The Cu²⁺–H RDF peaks at larger distances with respect to the corresponding oxygen peaks indicate that especially in the first shell the water molecules are fairly well dipole-oriented to obey the dominant ion–water interactions with their oxygen atoms pointing to the ionic center. Compared to the corresponding results of the classical MM simulations performed here and in earlier studies³⁷ employing three-body corrections, the following differences can be observed. The QM/MM simulation results in two distinctly separated hydration shells which are more compact and shifted to shorter distances than those of the MM simulation, where the first shell-peak is centered at 2.20 Å and the second shell covers the range from 3.0 to 5.3. The most prominent changes occur in the second hydration shell which appears less diffuse in the QM/MM than in the MM case. Both Cu²⁺–O RDF suggest the presence of a further, third hydration shell, indicating the central ion's influence up to 8 Å.

The mean coordination number obtained from the integration of the Cu–O RDF up to its first minimum amounts to 6 for the first hydration shell in agreement with the reference and earlier classical simulation studies.³⁷ The combined QM/MM approach leads, however, to deviating average coordination numbers for

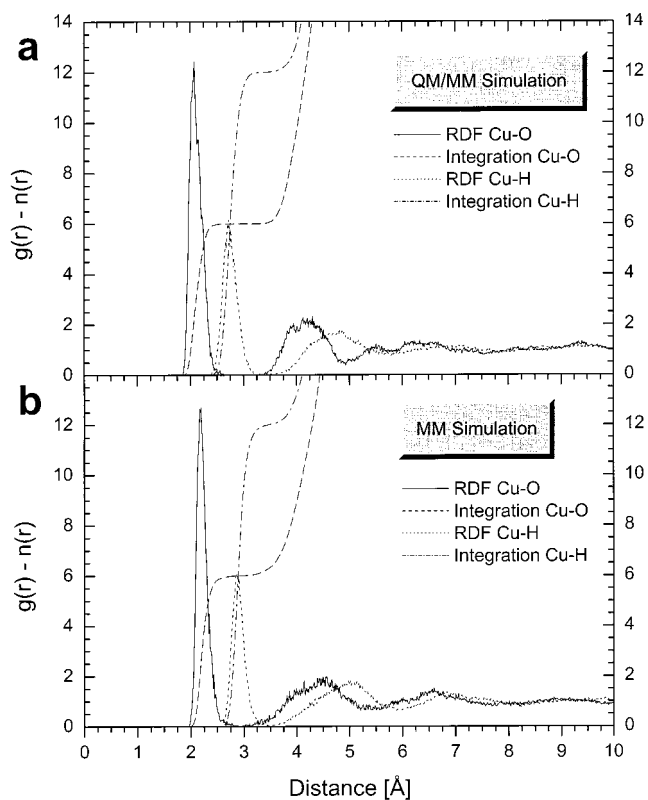


Figure 1. (a) Radial density functions and their running integration numbers for the QM/MM simulation. (b) Radial density functions and their running integration numbers for the simulation based on pair plus three-body interaction potentials for the Cu²⁺–H₂O interaction.

the second sphere, namely 14.5 second-shell ligands in contrast to 19 found previously³⁷ and 18.3 in the course of the classical reference simulation. Apparently, the ab initio treatment of the first hydration shell considerably influences the structure of the second solvation sphere as well, leading to a more ideally ordered hydrogen-bond network between water molecules across the first two hydration shells.

Figure 2 compares the actual species distribution of both shells for the classical three-body MM and the QM/MM simulation. While the ligands of the first sphere solely reorient in the course of the MC run without exchanging ligands with the outer hydration shell, the water molecules occupying the second shell are less strongly bound to the ionic center and thus more loosely organized, covering a wider range of possible coordination numbers.

While the knowledge of first-shell characteristics has increased remarkably during the last 2 decades,^{18,19} comparable experimental data for the second coordination sphere is rather scarce and usually limited to triple charged metal ions.^{74–78} X-ray data for Cu(II)^{79–81} indicate a second-shell maximum at 4.1–4.2 Å and between 7.6 and 11.6 water molecules to be contained in this shell. While the experimentally determined distance is in good agreement with the results found in this study, the corresponding coordination numbers seem to be considerably underestimated.

Ab initio studies⁸² predict the equatorial water molecules, which are more strongly bonded and polarized, to form stronger hydrogen bonds than the axial water molecules, thus increasing the JT distortion of the [Cu(H₂O)₆]²⁺ cluster in solution compared to the gas phase.^{5,19} These cooperative asymmetry effects from hydrogen bonds have been established experimentally by IR absorption spectroscopy,¹⁹ with an average $O_{\text{eq}}-O$ hydrogen bond distance of 2.74 Å and an $O_{\text{ax}}-O$ distance of

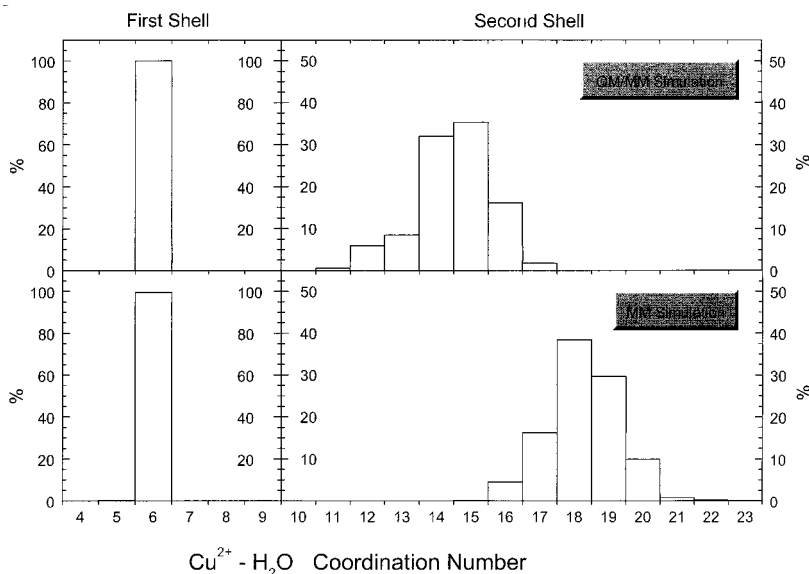


Figure 2. Coordination number distributions of the hydrated Cu^{2+} , comparing first and second shell for the QM/MM and the MM simulation.

2.88 Å, but are also recognized from the symmetric Raman stretching bands occurring at higher wavenumbers due to stronger Cu^{2+} – OH_2 bonds compared with the other divalent ions of the first transition period giving no rise to a JT distortion.¹⁰ The number of perturbed hydrogen bonds, as obtained from the IR measurements, indicates the formation of two hydrogen bonds per first-shell ligand, as is also expected from the simulation results presented here.

Jahn–Teller Effect. The full understanding of the JT effect in liquids, unlike in solids,⁸³ still poses some conceptual problems.⁸⁴ Experimental data related to the structure of the Cu^{2+} complex in aqueous electrolyte solutions at various concentrations are summarized in refs 15, 16, 19, 21, 85, and 86. Using the method of NDIS (neutron diffraction with isotopic substitution), the X-ray diffraction method or the extended X-ray absorption fine structure method, a (4 + 2) structural configuration for the $[\text{Cu}(\text{H}_2\text{O})_6]^{2+}$ complex has been found with a first peak at 1.96–2.01 Å assigned to the “equatorial” Cu – O_{eq} nearest-neighbor distance $r_{\text{CuO}(\text{eq})}$ and a further peak at 2.12–2.60 Å corresponding to the two longer “axial” Cu – O_{ax} bonds $r_{\text{CuO}(\text{ax})}$. The position of the second peak strongly depends on the method as well as on the counterion used in the experiment. The degree of $O_h \rightarrow D_{4h}$ distortion can be measured by the ratio $T = r_{\text{CuO}(\text{eq})}/r_{\text{CuO}(\text{ax})}$ which decreases from unity for an octahedral complex to values between 0.94 and 0.75 for aqueous solutions of copper salts at various concentrations.⁸⁵

NDIS measurements of the hydrogen position of the adjacent water ligands lead to “equatorial” Cu – D_{equ} distances of 2.62 and 2.65 Å and “axial” Cu – D_{ax} distances of 3.07 and 3.28, respectively,⁸⁷ depending on the copper salt. Compared to our results, this degree of distortion appears exaggerated, with the simulation leading to a Cu – H_{equ} value of 2.71 ± 0.26 Å and 2.86 ± 0.26 Å for the Cu – H_{ax} distance.

Detailed investigations of angular distributions lead to the picture in Figure 3 which displays the probability density of finding an angle φ (ligand(I)–center–ligand(II)) for both the combined QM/MM and the classical reference MM simulation, where the ligands are represented by their centers of mass CoM_i . The angular distribution ranges from 69° to 179° peaking at 88° and 172°, respectively, reflecting the basic octahedral structure of the hexahydrate complex. A similar result has already been obtained by the approximate treatment of three-body effects using the NNLC formalism³⁶ as well as by explicit

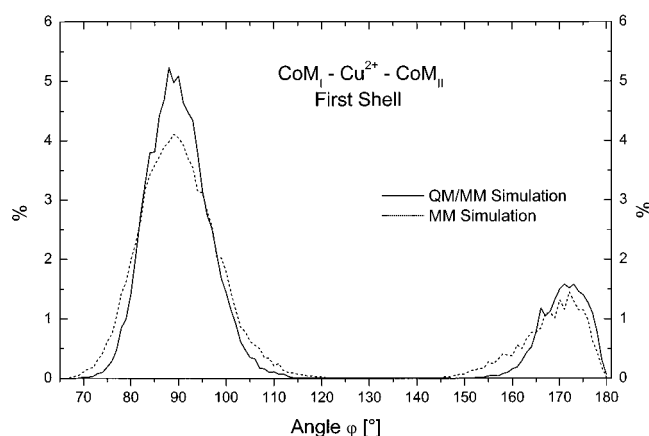


Figure 3. Comparison of bond angles φ [ligand(I)– Cu^{2+} –ligand(II)].

consideration of three-body potentials.³⁷ Except for a slightly increased compactness of the two peaks, this plot reveals no structural differences between the classical three-body MM and the quantum mechanically treated first hydration shell. Consequently, three-body potentials are suitable to correctly reproduce number and arrangements of the ligands around the central ion. However, more subtle structural properties require that n -body effects with $n > 3$ have to be included.

Monitoring the nearest ligands’ bond lengths during the course of the simulation led to Figure 4, where the development for the three pairs of opposite ligands is plotted. Accordingly, the hexaquo complex structure is continuously altered. Such a “dynamical” character of the JT distortion has been postulated on the basis of spectroscopic data^{22,87} and is fully confirmed by the results of our QM/MM simulation. Within this context it appears of particular interest that the changes of bond lengths always occur pairwise for ligands in opposite positions (1–2, 3–4, and 5–6 in Figure 4).

Distribution plots of the first-shell peak of the Cu^{2+} – O RDF for equatorial and axial ligands also reveal the JT distorted structure of the $[\text{Cu}^{2+}(\text{H}_2\text{O})_6]^{2+}$ complex. Figure 5 depicts the bond length distributions of the first-shell water ligands obtained from the QM/MM simulation. The average length of the longest bond in the solvate is 2.30 Å, and it can reach a maximum value of 2.64 Å, clearly separated from the distribution of all ligands which shows a remarkable tailing at longer distances

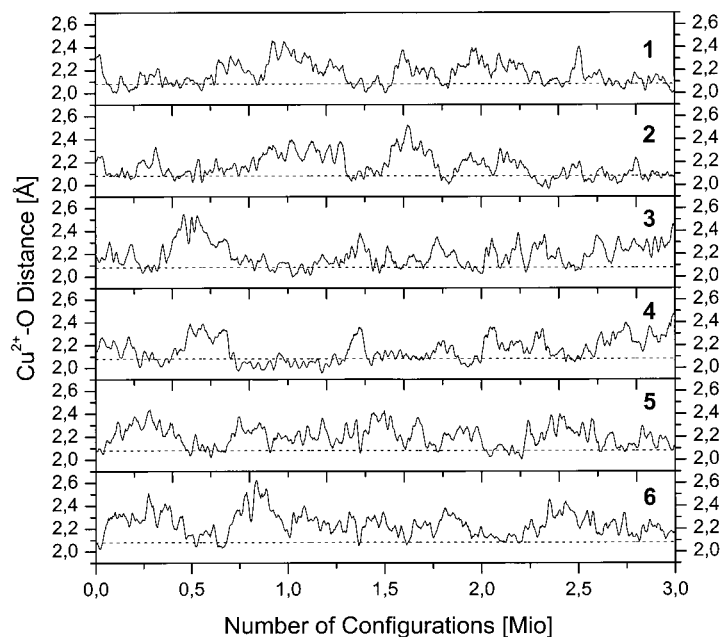


Figure 4. Comparison of the development of all Cu–O distances during the course of the simulation. The dotted horizontal line at 2.08 Å refers to the first-shell peak of the RDF for Cu–O (Figure 1).

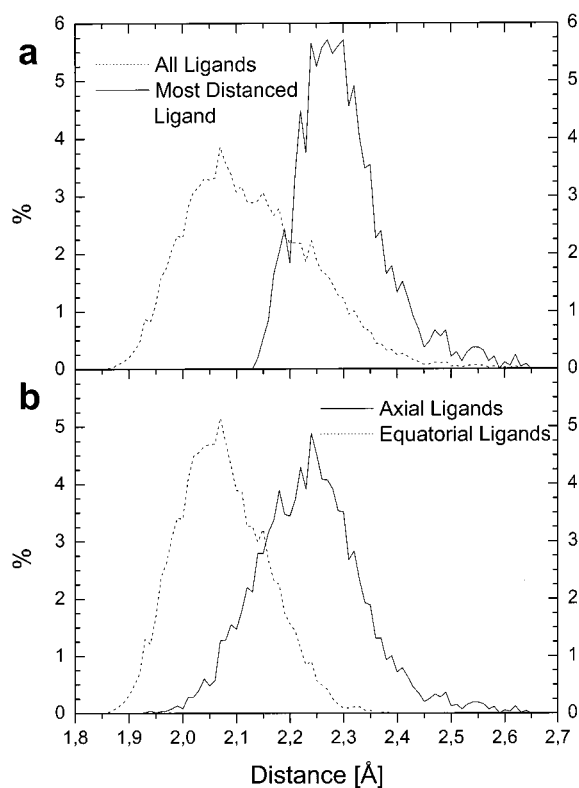


Figure 5. Bond length distribution Cu–O for all ligands versus the ligand with the most elongated bond axial ligands versus equatorial ligands.

caused by the “axial” ligands (Figure 5a). The comparison of “axial” and “equatorial” ligand distribution (Figure 5b) shows the $r_{\text{CuO}(\text{eq})}$ peak at 2.07 Å, while $r_{\text{CuO}(\text{ax})}$ has a mean value of 2.24 Å, well in agreement with experimental data. Likewise the ratio $T = 0.92$ calculated from the simulation results is within the experimentally determined range of this value.

Neutron diffraction experiments show deviations of 36° from the “ideal” linear dipole orientation of the adjacent water ligands.⁸⁸ However, since the model employed in the experi-

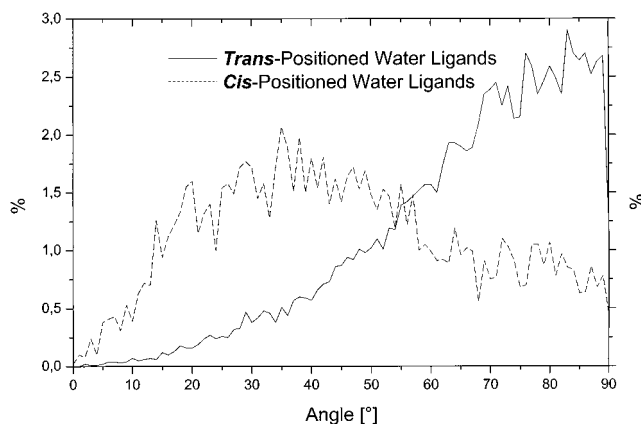


Figure 6. Comparison of the mutual ligand-plane orientation of cis- and trans-positioned water molecules, respectively.

mental study assumes a regular octahedral structure for the first hydration shell without JT distortion, the smaller deviations reaching a maximum plateau between 0° and 27° found in our QM/MM simulation appear more likely. The MM simulation results for these angles, however, are surely underestimated by reaching a maximum at 8°. Since the three-body potential has been optimized for equilibrium configurations with respect to dipole and water-plane orientation, the ligands preferably arrange themselves close to these pre-set conditions during the course of the classical potentials simulation. Figure 6 depicts further irregularities in the structure of the solvated $[\text{Cu}^{2+}(\text{H}_2\text{O})_6]^{2+}$ cluster compared to ab initio calculations and ligand field theory which predict the planes of opposite and adjacent water being orthogonal. Trans-positioned water molecules are predominantly configured in this way; the angular distribution between the ligand planes reaches a maximum value at 83°. In contrast, the same plot for planes of cis-positioned ligands covers a broader range of possible values reaching a less sharp maximum at 35°.

The hydration energy distributions for the solvated copper ion clearly show the importance of treating the strongly interacting area near the central ion by quantum mechanics. Figure 7 depicts the distribution of the energy (first shell) and

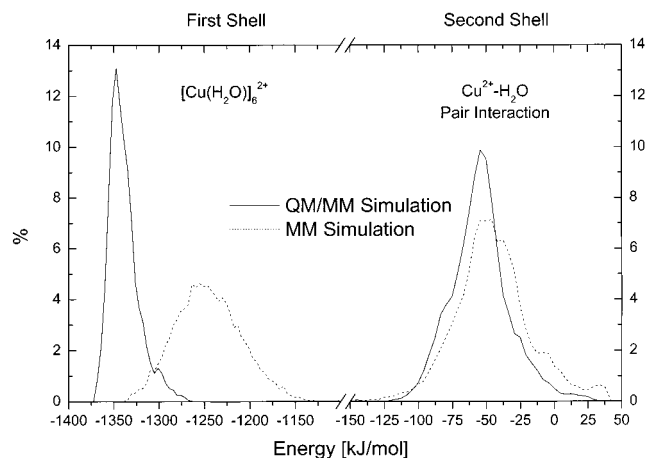


Figure 7. Energy distribution plot for the first and second hydration sphere of Cu^{2+} , showing the differences between the QM/MM and MM simulation results for the $[\text{Cu}(\text{H}_2\text{O})_6]^{2+}$ complex and the second shell pair interactions, respectively.

the pair interaction energy distribution for Cu^{2+} with H_2O ligands for the second shell for both the MM and the QM/MM simulation. As expected, advancing from a classical treatment of the first solvation shell to ab initio calculations leads to considerable changes concerning the energetics of this sphere. Lower energies and a peak contraction are found in accordance with the changes in the RDFs. Since the MM as well as the QM/MM simulation treat the second-shell region by the identical classical potentials the differences are not as pronounced as for the first solvation sphere. Nevertheless, a peak shift and contraction can be noticed which correspond to the reduction of the second-shell coordination number and its shorter distance to the first hydration sphere.

Experimental hydration enthalpies for copper ions have been determined in the range from -2470^{89} to -2100 kJ/mol,^{90,91} which can be compared to the hydration energies resulting from the simulations. Summing over all ion–water interactions in the system, the Cu^{2+} ion is stabilized by an energy of 3050 ± 67 kJ/mol in the case of the reference simulation with classical potentials and amounts to 3088 ± 96 kJ/mol for the QM/MM simulation. A better agreement with experimental results can be achieved by calculating the heat of hydration as energy difference between the simulations of water with and without ion under otherwise identical conditions. In this approach, both the classical and the QM/MM simulations lead to hydration energy values matching the experimental results, with 2096 ± 109 kJ/mol for pair plus three-body MM simulation and 2234 ± 105 kJ/mol for the QM/MM case.

5. Conclusion

The importance of sophisticated methods at ab initio level for a correct description of intermolecular interactions within the immediate environment of higher charged metal ions in solution, where higher-body effects considerably influence structure and energetics, is clearly confirmed. While traditional MC simulations employing pair and three-body potentials produce only rough or even wrong structural and energetical data, a more precise description of solvation phenomena can be achieved by the combined QM/MM approach implemented in this work, in particular for copper(II) in water where for the first time the JT distorted configuration of the $[\text{Cu}(\text{H}_2\text{O})_6]^{2+}$ complex could be reproduced on the basis of a condensed-system simulation.

Acknowledgment. Financial support by the Austrian Science Foundation (Project P11683-PHY) is gratefully acknowledged.

References and Notes

- (1) Cotton, F. A.; Wilkinson, G. W. *Advanced Inorganic Chemistry*, 5th ed.; Wiley: New York, 1988.
- (2) Sigel, H. *Metal Ions in Biological Systems*; M. Dekker: New York, 1974; Vol. 1.
- (3) Williams, R. J. P. *J. Chem. Soc., Dalton Trans.* **1991**, 539.
- (4) Williams, R. J. P. *Coord. Chem. Rev.* **1990**, *100*, 573.
- (5) Veillard, H. *J. Am. Chem. Soc.* **1977**, *99*, 7194.
- (6) Beagley, B.; Eriksson, A.; Lindgren, J.; Persson, I.; Pettersson, L. G. M.; Sandström, M.; Wahlgren, U.; White, E. W. *J. Phys.: Condens. Matter* **1989**, *1*, 2395.
- (7) Åkesson, R.; Pettersson, L. G. M.; Sandström, M.; Wahlgren, U. *J. Phys. Chem.* **1992**, *96*, 150.
- (8) Liedl, K. R.; Rode, B. M. *Chem. Phys. Lett.* **1992**, *197*, 181.
- (9) Åkesson, R.; Pettersson, L. G. M.; Sandström, M.; Siegbahn, P. E. M.; Wahlgren, U. *J. Phys. Chem.* **1992**, *96*, 10773.
- (10) Åkesson, R.; Pettersson, L. G. M.; Sandström, M.; Siegbahn, P. E. M.; Wahlgren, U. *J. Phys. Chem.* **1993**, *97*, 3765.
- (11) Åkesson, R.; Pettersson, L. G. M.; Sandström, M.; Wahlgren, U. *J. Am. Chem. Soc.* **1994**, *116*, 8691.
- (12) Åkesson, R.; Pettersson, L. G. M.; Sandström, M.; Wahlgren, U. *J. Am. Chem. Soc.* **1994**, *116*, 8705.
- (13) Waizumi, K.; Ohtaki, H.; Masuda, H.; Fukushima, N.; Watanabe, Y. *Chem. Lett.* **1992**, 1489.
- (14) Fukushima, N.; Waizumi, K. *Chem. Express* **1993**, *8*, 265.
- (15) Johansson, G. *Adv. Inorg. Chem.* **1992**, *39*, 159.
- (16) Neilson, G. W.; Enderby, J. E. *Adv. Inorg. Chem.* **1989**, *34*, 195.
- (17) Neilson, G. W.; Ansell, S.; Wilson, J. *Z. Naturforsch.* **1995**, *50a*, 247.
- (18) Lincoln, S. F.; Merbach, A. E. Substitution Reactions of Solvated Metal Ions. *Advances in Inorganic Chemistry*; Academic Press: New York, 1995; Vol. 42, p 1.
- (19) Beagley, B.; Eriksson, A.; Lindgren, J.; Persson, I.; Pettersson, L. G. M.; Sandström, M.; Wahlgren, U.; White, E. W. *J. Phys.: Condens. Matter* **1989**, *1*, 2395.
- (20) Ohtaki, H.; Radnai, T. *Chem. Rev.* **1993**, *93*, 1157.
- (21) Okan, S. E.; Salmon, P. S. *Mol. Phys.* **1995**, *85*, 981.
- (22) Powell, D. H.; Helm, L.; Merbach, A. E. *J. Chem. Phys.* **1991**, *95*, 9258.
- (23) Powell, D. H.; Furrer, P.; Pittet, P. A.; Merbach, A. E. *J. Phys. Chem.* **1995**, *99*, 16622.
- (24) Stace, A. J.; Walker, N. R.; Firth, S. *J. Am. Chem. Soc.* **1997**, *119*, 10239.
- (25) Limtrakul, J. P.; Probst, M. M.; Rode, B. M. *J. Mol. Struct. Theochem.* **1985**, *23*, 121.
- (26) Bopp, P.; Okada, I.; Ohtaki, H.; Heinzinger, K. *Z. Naturforsch., Teil A* **1985**, *40*, 116.
- (27) Spohr, E.; Pálinkás, G.; Heinzinger, K.; Bopp, P.; Probst, M. M. *J. Phys. Chem.* **1988**, *92*, 6754.
- (28) Clementi, E.; Kistenmacher, H.; Kolos, W.; Romano, S. *Theor. Chim. Acta* **1980**, *55*, 257.
- (29) Lybrand, T. P.; Kollman, P. A. *J. Chem. Phys.* **1985**, *83*, 2923.
- (30) Probst, M. M.; Spohr, E.; Heinzinger, K. *Chem. Phys. Lett.* **1989**, *161*, 405.
- (31) Probst, M. M.; Spohr, E.; Heinzinger, K. *Mol. Simul.* **1991**, *7*, 43.
- (32) González-Lafont, A.; Lluch, J. M.; Olivía, A.; Bertrán, J. *Chem. Phys.* **1987**, *111*, 241.
- (33) Curtiss, L. A.; Halley, J. W.; Hautman, J.; Rahman, A. *J. Chem. Phys.* **1987**, *86*, 2319.
- (34) Bounds, D. G. *Mol. Phys.* **1985**, *54*, 1335.
- (35) Natália, M.; Cordeiro, M. N. D. S.; Ignaczak, A.; Gomes, J. A. N. *J. Chem. Phys.* **1993**, *176*, 97.
- (36) Rode, B. M.; Islam, S. M. *Z. Naturforsch., Part A* **1991**, *46*, 357.
- (37) Texler, N. R.; Rode, B. M. *J. Phys. Chem.* **1995**, *99*, 15714.
- (38) Natália, M.; Cordeiro, M. N. D. S.; Gomes, J. A. N. *F. J. Comput. Chem.* **1993**, *14*, 629.
- (39) Cordeiro, M. N. D. S.; Gomes, J. A. N. F.; González-Lafont, A.; Lluch, J. M.; Bertrán, J. *Chem. Phys.* **1990**, *141*, 379.
- (40) Rode, B. M.; Islam, S. M.; Yongyai, Y. *Pure Appl. Chem.* **1991**, *63*, 1725.
- (41) Rode, B. M.; Islam, S. M. *J. Chem. Soc., Faraday Trans. 1* **1992**, *88*, 417.
- (42) Yongyai, Y.; Kokpol, S.; Rode, B. M. *Chem. Phys.* **1991**, *156*, 403.
- (43) Yongyai, Y.; Kokpol, S.; Rode, B. M. *J. Chem. Soc., Faraday Trans. 1992, *88*, 1537.*
- (44) Ortega-Blake, I.; Novaro, O.; Les', A.; Rybak, S. *J. Chem. Phys.* **1982**, *76*, 5405.
- (45) Hannongbua, S.; Kerdcharoen, T.; Rode, B. M. *J. Chem. Phys.* **1992**, *96*, 6945.

- (46) Marini, G. W.; Texler, N. R.; Rode, B. M. *J. Chem. Phys.* **1996**, *100*, 6808.
- (47) Dietrich, J.; Corongiu, G.; Clementi, E. *Chem. Phys. Lett.* **1984**, *112*, 426.
- (48) Warshel, A.; Levitt, M. *J. Mol. Biol.* **1976**, *103*, 277.
- (49) Bash, P. A.; Field, M. J.; Karplus, M. *J. Am. Chem. Soc.* **1987**, *109*, 8092.
- (50) Field, M. J.; Bash, P. A.; Karplus, M. *J. Comput. Chem.* **1990**, *11*, 700.
- (51) Mordasini, T. Z.; Thiel, W. *Chimia* **1998**, *52*, 288.
- (52) Gao, J. In *Review of Computational Chemistry*; Lipkowitz, K. B., Boyd, D. B., Eds.; VCH: New York, 1995; Vol. 7, 119.
- (53) Gao, J. *J. Chem. Phys.* **1992**, *96*, 537.
- (54) Wie, D.; Salahub, D. R. *Chem. Phys. Lett.* **1994**, *224*, 291.
- (55) Tunón, I.; Martins-Costa, T. C.; Millot, C.; Ruiz-Lopez, M. F.; Rivail, J. L. *J. Comput. Chem.* **1996**, *17*, 19.
- (56) Gao, J. *J. Comput. Chem.* **1997**, *18*, 1061.
- (57) Cummings, P. L.; Gready, J. L. *J. Comput. Chem.* **1997**, *18*, 1496.
- (58) Kercharoen, T.; Liedl, K. R.; Rode, B. M. *Chem. Phys.* **1996**, *211*, 313.
- (59) Tongraar, A.; Liedl, K. R.; Rode, B. M. *J. Phys. Chem. A* **1997**, *101*, 6299.
- (60) Tongraar, A.; Liedl, K. R.; Rode, B. M. *Chem. Phys. Lett.* **1998**, *286*, 56.
- (61) Stanton, R. V.; Hartsough, D. S.; Merz, Jr, K. M. *J. Phys. Chem.* **1993**, *97*, 11868.
- (62) Truong, T. N.; Stefanovich, E. V. *Chem. Phys.* **1996**, *218*, 31.
- (63) Rode, B. M.; Heinzle, M. G.; Marini, G. W. *MC98*; **1998**.
- (64) Brooks, B. R.; Bruccoleri, R. E.; Olafson, B. D.; States, D. J.; Swaminathan, S.; Karplus, M. *J. Comput. Chem.* **1983**, *4*, 187.
- (65) Frisch, M. J.; Trucks, G. W.; Schlegel, H. B.; Gill, P. M. W.; Johnson, B. G.; Robb, M. A.; Cheeseman, J. R.; Keith, T.; Petersson, G. A.; Montgomery, J. A.; Raghavachari, K.; Al-Laham, M. A.; Zakrzewski, V. G.; Ortiz, J. V.; Foresman, J. B.; Cioslowski, J.; Stefanov, B. B.; Nanayakkara, A.; Challacombe, M.; Peng, C. Y.; Ayala, P. Y.; Chen, W.; Wong, M. W.; Andres, J. L.; Replogle, E. S.; Gomperts, R.; Martin, R. L.; Fox, D. J.; Binkley, J. S.; Defrees, D. J.; Baker, J.; Stewart, J. P.; Head-Gordon, M.; Gonzalez, C.; Pople, J. A. *Gaussian 94*, revision E.1; Gaussian, Inc., Pittsburgh, PA, 1995.
- (66) Frisch, M. J.; Trucks, G. W.; Schlegel, H. B.; Scuseria, G. E.; Robb, M. A.; Cheeseman, J. R.; Zakrzewski, V. G.; Montgomery, J. A., Jr.; Stratmann, R. E.; Burant, J. C.; Dapprich, S.; Millam, J. M.; Daniels, A. D.; Kudin, K. N.; Strain, M. C.; Farkas, O.; Tomasi, J.; Barone, V.; Cossi, M.; Cammi, R.; Mennucci, B.; Pomelli, C.; Adamo, C.; Clifford, S.; Ochterski, J.; Petersson, G. A.; Ayala, P. Y.; Cui, Q.; Morokuma, K.; Malick, D. K.; Rabuck, A. D.; Raghavachari, K.; Foresman, J. B.; Cioslowski, J.; Ortiz, J. V.; Stefanov, B. B.; Liu, G.; Liashenko, A.; Piskorz, P.; Komaromi, I.; Gomperts, R.; Martin, R. L.; Fox, D. J.; Keith, T.; Al-Laham, M. A.; Peng, C. Y.; Nanayakkara, A.; Gonzalez, C.; Challacombe, M.; Gill, P. M. W.; Johnson, B.; Chen, W.; Wong, M. W.; Andres, J. L.; Gonzalez, C.; Head-Gordon, M.; Replogle, E. S.; Pople, J. A. *Gaussian 98*, revision A.3; Gaussian, Inc., Pittsburgh, PA, 1998.
- (67) Jancsó, G.; Heinzinger, K. Z. *Naturforsch., Part A* **1985**, *40*, 1235.
- (68) Matsuoka, O.; Clementi, E.; Yoshimine, M. *J. Phys. Chem.* **1976**, *64*, 1351.
- (69) Rode, B. M. *J. Phys. Chem.* **1992**, *96*, 4170.
- (70) Schafer, A.; Horn, H.; Ahlrichs, R. *J. Chem. Phys.* **1992**, *97*, 2571.
- (71) Dunning, T. H., Jr.; Hay, P. J. In *Modern Theoretical Chemistry*; Schaefer, H. F., III, Ed.; Plenum: New York, 1976; p 1.
- (72) Kuchitsu, K.; Morino, Y. *Bull. Chem. Soc. Jpn.* **1965**, *38*, 814.
- (73) Texler, N. R.; Rode, B. M. *Chem. Phys.* **1997**, *222*, 281.
- (74) Bergström, P. A.; Lindgren, J. *J. Chem. Phys.* **1991**, *95*, 7650.
- (75) Munoz-Paez, A.; Marcos, E. S. *J. Am. Chem. Soc.* **1992**, *114*, 6931.
- (76) Munoz-Paez, A.; Pappalardo, R. R.; Marcos, E. S. *J. Am. Chem. Soc.* **1995**, *117*, 11710.
- (77) Bányai, I.; Glaser, J.; Read, M. C.; Sandström, M. *Inorg. Chem.* **1995**, *34*, 2423.
- (78) Bleuzen, A.; Foglia, F.; Furet, E.; Helm, L.; Merbach, A. E.; Weber, J. *J. Am. Chem. Soc.* **1996**, *118*, 12777.
- (79) Magini, M. *Inorg. Chem.* **1982**, *21*, 1535.
- (80) Musinu, A.; Paschina, G.; Piccaluga, G.; Magini, M. *Inorg. Chem.* **1983**, *22*, 1184.
- (81) Licheri, G.; Musinu, A.; Paschina, G.; Piccaluga, G.; Sedda, A. F. *J. Chem. Phys.* **1984**, *80*, 5308.
- (82) Hermansson, K.; Olovsson, I.; Lunell, S. *Theor. Chim. Acta* **1984**, *64*, 265.
- (83) Perlin, Y. E.; Wagner, M. *The Dynamical Jahn–Teller Effect in Localised Systems*; Elsevier: Amsterdam, 1984.
- (84) Curtiss, L.; Halley, J. W.; Wang, X. R. *Phys. Rev. Lett.* **1992**, *69*, 2435.
- (85) Okan, S. E.; Salmon, P. S. *Mol. Phys.* **1995**, *85*, 981.
- (86) Neilson, G. W.; Broadbent, R. D.; Howell, I.; Tromp, R. H. *J. Chem. Soc., Faraday Trans.* **1993**, *16*, 89.
- (87) Salmon, P. S.; Howell, W. S.; Mills, R. *J. Phys. C* **1987**, *20*, 5727.
- (88) Neilson, G. W.; Newsome, J. R.; Sandström, M. *J. Chem. Soc., Faraday Trans. 2* **1981**, *77*, 1245.
- (89) Bockris, J. O'M.; Redy, A. K. N. *Modern Electrochemistry I*; Plenum: New York, 1970.
- (90) Friedman, H. L.; Krishnan, C. V. In *Water, A Comprehensive Treatise*; Franks, F., Ed.; Plenum: New York, London, 1973; Vol. 3.
- (91) Smith, D. W. *J. Chem. Educ.* **1977**, *54*, 540.